Investigation of the figure of merit for filters with a single nanofiber layer on a substrate

Jing Wang*, Seong Chan Kim, David Y.H. Pui

Particle Technology Laboratory, Department of Mechanical Engineering, University of Minnesota, Minneapolis, MN, USA

Abstract

We investigate filters composed of a layer of nanofibers on a substrate made of micrometer fibers and compare the performance of such nanofiber media to conventional micrometer fibrous filters. The performance of the nanofiber filters is evaluated using the figure of merit, which represents the ratio between the filtration efficiency and the pressure drop. Filtration tests were performed on four samples with different nanofiber solidities. As the nanofiber solidity increases, the filtration efficiency and the pressure drop both increase. We develop a numerical model to simulate the nanofiber filters. When the nanofiber solidity is appropriately adjusted, the pressure drop computed from the model is in good agreement with experimental results. Filtration efficiency for the nanofibers due to interception, inertial impaction and diffusion can be computed from the model. The simulation results are in good agreement with experiments for 20–780 nm particles but discrepancies exist for particles smaller than 20 nm. Our results show that nanofiber filters have better figure of merit for particles larger than about 100 nm compared to conventional fiberglass filters. For particles smaller than 100 nm, nanofiber filters do not perform better than conventional fiberglass filters.
© 2007 Elsevier Ltd. All rights reserved.

Keywords: Nanofiber filters; Figure of merit

1. Introduction

Nanofiber media has emerged as a promising media which can provide a greater filtration efficiency and higher performance than conventional fibers. The non-woven industry generally considers nanofibers as having a diameter of less than 0.5 μm (George, 2007). A number of companies are developing filtration media using nanofibers, such as Ultra-Web® and Fibra-Web® nanofiber media technology by Donaldson Company, Finetex Mats ™ by Finetex Technology Inc., and AMSOIL Ea Air Filters. Subbiah, Bhat, Tock, Parameswaran, and Ramkumar (2005), George (2007) and Ellison, Phatak, Giles, Macosko, and Bates (2007) focused on manufacturing techniques for nanofibers. Graham et al. (2002), Gradoń, Bałazy, and Podgórski (2006), Kalayci, Ouyang, and Graham (2006), Kim et al. (2006), Podgórski, Bałazy, and Gradoń (2006) and Barhate and Ramakrishna (2007) investigated production and filtration performances of nanofibers.

---

* Corresponding author.

E-mail address: wangj@aem.umn.edu (J. Wang).

Filtration efficiency and pressure drop are the most important criterions for evaluating filters. Filtration efficiency is equal to $1 -$ penetration, where the penetration P is defined as

$$P = \frac{\text{particle concentration downstream of the filter}}{\text{particle concentration upstream of the filter}}. \tag{1}$$

The relation between the penetration P and the single-fiber efficiency E can be written as

$$P = \exp\left(-\frac{4\alpha E t}{\pi d_{\mathrm{f}}(1 - \alpha)}\right), \tag{2}$$

where t is the filter thickness, α is the filter solidity and d_{f} is the fiber diameter.

The effects of the fiber size can be predicted from classical filtration theories. Let us consider the most penetrating particle size (MPPS) and the minimum single-fiber efficiency E^*. As the fiber size decreases, the MPPS decreases and E^* becomes greater (Hinds, 1998; Lee & Liu, 1980). The pressure drop is inversely proportional to the square of the fiber diameter for continuum regime (Davies, 1973). The increase of the pressure drop with decreasing fiber diameter is less steep for nanofibers due to the slip effect. Nevertheless, Δp increases significantly when the fiber diameter decreases even in the slip regime (Brown, 1993, p. 61) when the solidity is held constant. The classical filtration theories cited here indicate that the nanofiber media can improve the filtration efficiency, but the greater pressure drop may be a concern. To evaluate the overall performance, a useful criterion is the figure of merit Q (also know as the quality factor, see Brown, 1993) which is defined as

$$Q = -\ln(P)/\Delta p. \tag{3}$$

Since $-\ln(P)$ provides a measure of the filter efficiency, the figure of merit represents the ratio between the efficiency and the pressure drop Δp. Good filters give high efficiency and low pressure drop, thus larger values of Q indicate better quality of the filters.

The main objective of this study is to evaluate the filtration performance of nanofiber filters and investigate if nanofiber media can improve the figure of merit compared to conventional micrometer fibrous filter media. Podgórski et al. (2006) showed improved figure of merit for the MPPS when fibers with the mean diameter in the range of 0.74–1.41 μm were used. The nanofibers in our samples have a diameter of about 0.15 μm. In Section 2, we present the experimental results for the filtration efficiency and pressure drop, which are necessary in calculation of the figure of merit. In Section 3, a numerical model for the nanofiber filters is presented and validated using the experimental data. The numerical model provides a tool to easily change the parameters such as nanofiber diameter and solidity and evaluate their effects on the figure of merit. In Section 4, the figure of merit of nanofiber filters is presented and compared to that of conventional fiberglass filter media. The effect of nanofiber solidity on the figure of merit is also discussed.

2. Experimental evaluation

Our filter testing system has been detailed in the previous works (Kim, Harrington, & Pui, 2007; Wang, Chen, & Pui, 2007) and will only be briefly described here. In this study, penetration tests have been performed using 3–20 nm silver particles, 20–300 nm NaCl particles and 780 nm PSL particles. Silver particles were generated by heating a pure silver powder source in an electric furnace. The silver particles were then classified in a nanodifferential mobility analyzer (nano-DMA) and neutralized before being sent to challenge the filters. NaCl particles were generated by a collison atomizer and classified by a DMA. PSL particles were generated by a collison atomizer with a monodisperse PSL colloidal suspension. The particle concentrations upstream and downstream of the filter were measured by an ultrafine condensation particle counter (UCPC) after the particle concentrations were stable.

Tests were performed on nanofiber filters composed of a layer of nanofibers on a substrate made of micrometer fibers. The nanofibers capture contaminants on the surface of the filter; the resulting dust cake is easily cleaned off during cleaning cycles, ensuring high filtration efficiency and long filter life. The substrate provides necessary support for the fragile nanofiber layer. The SEM images in Fig. 1 show the structure clearly. Four different samples with different nanofiber solidities are tested; Sample A has the highest solidity whereas Sample D has the lowest one. The substrates in the four samples are the same. We can define an effective nanofiber solidity α (see Eq. (4) in Section 3), which represents the solid fraction in the nanofiber layer. We determine the values of α by matching the pressure drop
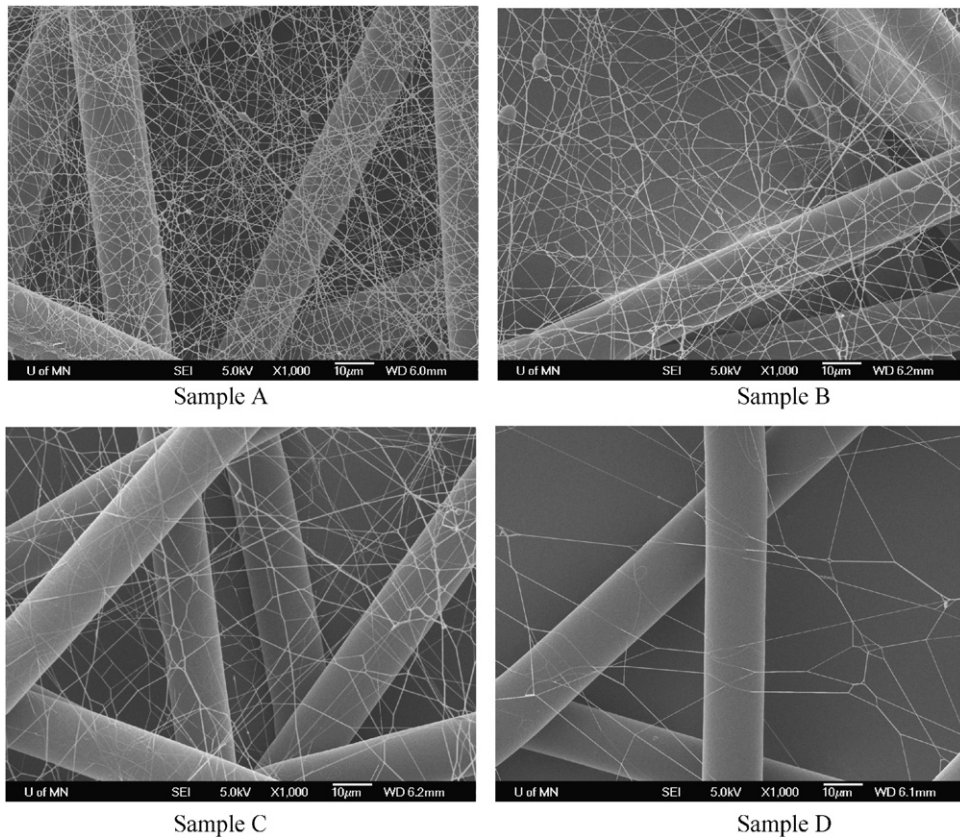
Fig. 1. SEM images for the nanofiber filters composed of a layer of nanofibers on a substrate made of micrometer fibers. The solidity of the nanofibers decreases from Sample A to Sample D.

Table 1
The values of the effective nanofiber solidity α for the four samples

Sample ID	A	B	C	D	Substrate
Nanofiber solidity α	0.134	0.104	0.059	0.034	0
Efficiency (%)	80.01	58.84	38.40	21.36	4.28
Pressure drop (Pa)	29.4	14.7	7.7	4.0	2.2

The pressure drop and filtration efficiency for 0.78 μm PSL particles measured at the face velocity of 10 cm/s are also listed.

measured from experiments to those computed from simulations (see Fig. 5). The values of α are reported in Table 1. We assign $\alpha = 0$ when the bare substrate is considered because no nanofiber layer is involved. The pressure drop and the filtration efficiency of 780 nm PSL particles at a face velocity of 10 cm/s are listed in Table 1. The nanofiber layer can significantly improve the filtration efficiency. Even with a sparse nanofiber layer as in Sample D, the efficiency is five times that of the substrate. Sample A has the highest efficiency at 80% but the pressure drop is more than 10 times higher than the substrate. The improved efficiency comes with the cost of high pressure drop.

The pressure drop is measured at six face velocities up to 40 cm/s and the results are plotted in Fig. 2. The linear relationship between the pressure drop and the face velocity is in accordance with the Darcy's law. Penetration tests have been performed using 3–20 nm silver particles, 20–300 nm NaCl particles and 780 nm PSL particles. The data for penetration vs. the particle size are plotted in Fig. 3. The curves take a typical "Λ" shape, with the MPPS at about 100–200 nm. The value of the MPPS decreases as the nanofiber solidity increases; it is approximately 200 nm for the substrate, 100 nm for Sample C and 75 nm for Sample A. The nanofiber solidity increases from Sample D to Sample A, therefore the penetration decreases from D to A.
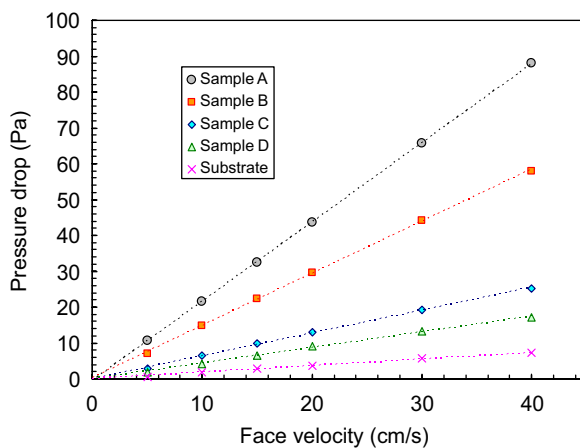
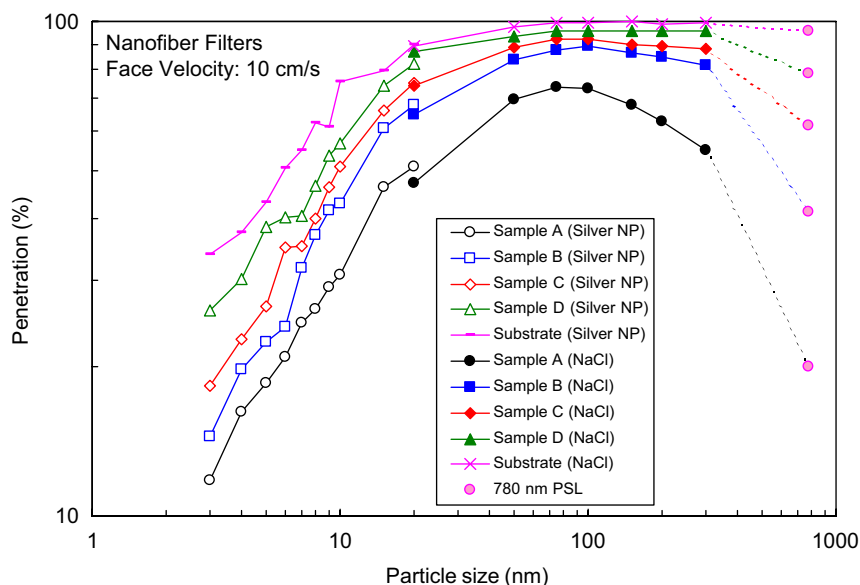Fig. 2. The pressure drop as a function of the face velocity for the nanofiber filters.

Fig. 3. Penetration vs. the particle size for nanofiber filters. Silver nanoparticles (NP) in the range of 3–20 nm, NaCl in the range of 20–300 nm and 780 PSL particles are tested. The face velocity is 10 cm/s.

3. Numerical simulation of nanofiber filters

We have developed a numerical model for fibrous filtration using the computational fluid dynamics code FLUENT. To simulate the nanofiber filters, we need to take the specific structure of the nanofiber Samples A–D into account. The two-dimensional model, illustrated in Fig. 4, represents a cross section of the filter. The single-layer nanofibers are described by evenly distributed circular fibers, whereas the substrate is modeled by a porous jump media, which is a simplified boundary condition represented by a one-dimensional line in FLUENT. The porous jump media gives the pressure drop across the substrate and ignores the detailed structure inside. The parameters used in the porous jump media, including the permeability (1.465×10^{-10} m^2) and thickness of the substrate (0.15 mm), are both determined using experimental data. The two-dimensional model is a simplified approximation which ignores the different orientations of nanofibers and details in the substrate. This approach allows us to focus on the nanofibers and simplify the calculation.
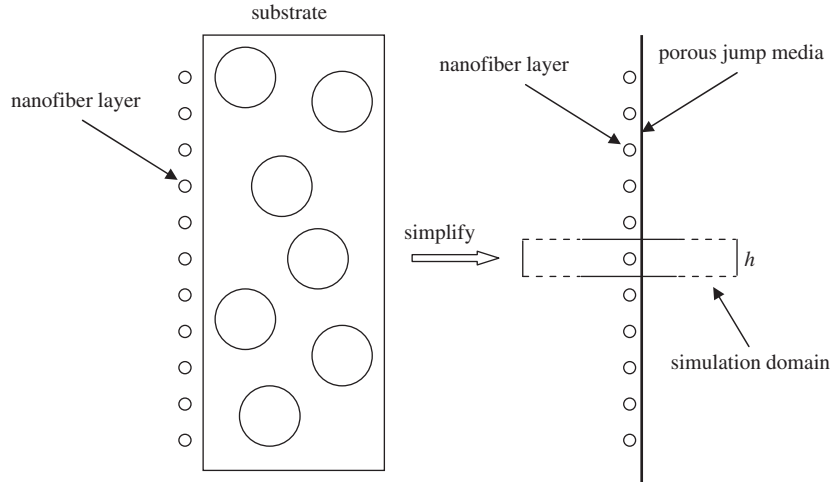
Fig. 4. The numerical model for the nanofiber media composed of one layer of nanofibers and a substrate made of micrometer fibers.
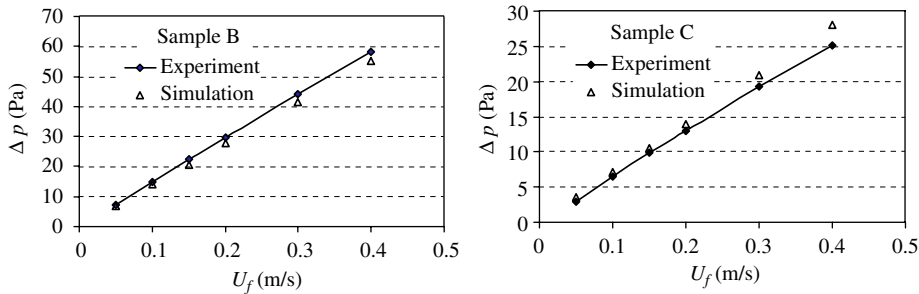

Fig. 5. Comparison of the pressure drop across the nonofiber filters at different face velocities from experiments and the numberical model.

Since the nanofibers have the same diameter and are distributed evenly in our model, we can consider only one fiber in our rectangular simulation domain (see Fig. 4). The left side of the simulation domain is the inlet of the flow, where the flow velocity is prescribed. The right side of the domain is the outlet, where the derivative of the velocity normal to the outlet is set to zero. For the upper and lower boundaries of the domain, periodic boundary condition is applied. The diameter of the nanofibers is determined from SEM images to be $d_f = 150$ nm. The Knudsen number is $Kn = 2\lambda/d_f = 0.88$ under standard conditions, where λ is the mean free path of air. This Knudsen number indicates that molecular effects of gas are important. We use the slip condition (Eq. (3.60) in Brown, 1993) on the surface of the nanofibers. Kirsch and Stechkina (1978) stated that results using the slip condition may be applied up to $Kn \sim 1$. The distances from the inlet and outlet to the nanofiber are about 25 times of the fiber diameter, which is sufficiently large so that upstream and downstream conditions do not unduly affect the simulation results (Liu, 1993). The distance h between two nanofibers, which is also the width of the simulation domain, determines the solidity α, which is defined as

$$\alpha = \frac{\pi d_f^2}{(4hd_f)}. \tag{4}$$

It should be noted that the solidity is defined for the nanofiber layer only and the substrate is not involved.

The flow field in the simulation domain was computed and the pressure drop was obtained as the difference between the pressures at the inlet and outlet. We adjusted the solidity to match the pressure drop measured in experiments. We used $\alpha = 0.134, 0.104, 0.059$ and 0.034 for Samples A, B, C, and D, respectively. Fig. 5 shows that the pressure drop computed from the model increases linearly with the face velocity. The pressure drop from experiments also has a

Table 2
Simulation results for Sample C for the efficiency due to inertial impaction and interception E_{I+R}, the efficiency due to diffusion E_D, and the total penetration across the composite filter P

Particle size (nm)	5	20	50	100	300	780
E_{I+R}	Ignored	0.02	0.127	0.328	1.39	4.77
E_D	19.2	3.0	0.851	0.388	0.145	0.076
P (simulation) (%)	9.3	70.5	89.9	93.8	87.9	65.1
P (experiment) (%)	26.6	75	88.5	92.2	88.1	61.6

The simulation results for P are compared to those from experiments.

linear relation with the face velocity. Since we adjust the solidity in our model to match the experimental results, the two linear curves agree well with each other as expected.

We computed the filtration efficiency due to inertial impaction and interception by use of the discrete phase model in FLUENT. This model calculates the trajectories of particles using a Lagrangian formulation that includes the particle inertia and hydrodynamic drag. Since we are considering the efficiency due to inertial impaction and interception, the gravity forces and random forces due to Brownian motion are not included. The particles are considered to be point masses in the discrete phase model and the size is neglected. To overcome this defect, we wrote a user defined function (UDF) to take the particle size into account. The UDF compares the particle radius with the distance from the center of the particle to the surface of the fiber, and determines whether the particle is captured or not. Single particles were released at the inlet from different distances from the horizontal line going through the center of the fiber. The fate of the particle (captured or escape) was determined and the critical distance Y below which the particle was captured by the fiber was obtained. The efficiency was obtained as $Y/(d_f/2)$. The efficiency computed using this approach was due to the combined effects of inertial impaction and interception, which was denoted as E_{I+R}.

The efficiency due to diffusion may be obtained by solving the convective diffusion equation for the particle concentration (Friedlander, 1957; Lee & Liu, 1982; Natanson, 1957a,b; Stechkina, 1966, among others). The domain of simulation was the same as for the flow. The particle concentration was prescribed at the inlet. Particles were assumed to be captured as they contacted the fiber and were permanently removed from the aerosol stream, thus the particle concentration was zero on the surface of the fiber. The periodic condition was imposed on the upper and lower boundaries of the domain. The derivative of the particle concentration normal to the outlet was set to zero. After the convective diffusion equation was solved, the distribution of the particle concentration was obtained. The ratio between the particle concentrations at the outlet and inlet was the penetration when diffusion was considered. This penetration was converted to the efficiency due to diffusion E_D using Eq. (2). The filter thickness in Eq. (2) was equal to the fiber diameter, since only one layer of fiber was considered. We computed the total efficiency as $E_{I+R} + E_D$, and obtained the penetration across the nanofiber layer using Eq. (2) and the total efficiency.

Our simulation gives the penetration for the nanofiber layer, not for the substrate because the detailed structure in the substrate is ignored. To obtain the total penetration for the composite filter, we assume (i) the nanofiber layer and the substrate act independently and in series to capture particles; (ii) the penetration through the substrate in the composite filter is the same as that through the bare substrate. Based on these assumptions, we can compute the total penetration as

$$P = P^N \times P^S, \tag{5}$$

where P^N and P^S are the penetrations through the nanofiber layer and the substrate, respectively. We compute P^N from simulation and measure P^S in experiments, then obtain P using Eq. (5). We list the simulation results for Sample C in Table 2. The results for Samples A, B, C and D are plotted in Fig. 6 and compared to experimental data. Excellent agreement is obtained for 20–780 nm particles. The key parameters for filter evaluation, the maximum penetration and the MPPS, are correctly predicted for each sample. These results provide solid validation of our numerical model. It is also noted that the penetrations measured in experiments are higher than those predicted by the numerical model for particles smaller than 20 nm. More discussion about this discrepancy will be given at the end of this section.

Analytical expressions for filtration efficiencies and pressure drop with slip effect exist in the literature (Kirsch & Stechkina, 1978; Brown, 1993). Most of these expressions are based on the Kuwabara flow field with the slip condition. Our numerical model is different from the analytical expressions in several aspects. The geometry considered in our
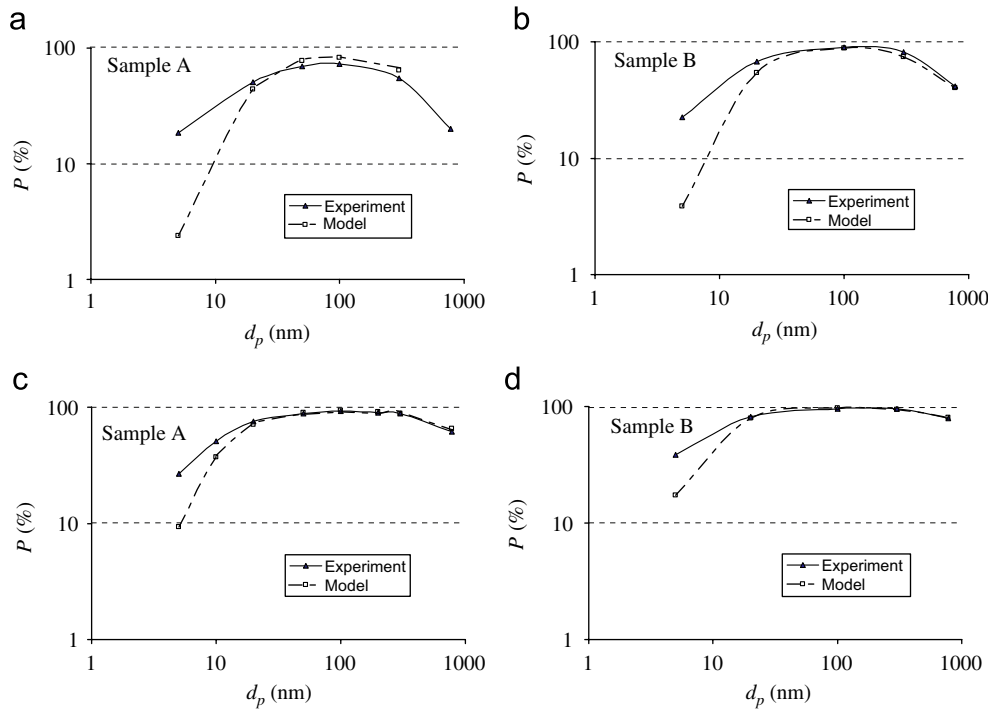
Fig. 6. Penetration P vs. particle size d_p for nanofiber Samples A–D. The results from experiments and the numerical model are compared.

model involves a layer of fibers in front of a porous jump media. In the Kuwabara flow, a fiber is enclosed in a circular cell and the cell boundary is used to represent the influence of neighbor fibers of the same size in all directions. The geometry in our model is closer to the real structure of the nanofiber samples in this study. We impose the inlet and outlet conditions far away from the fiber. In the Kuwabara flow, artificial boundary conditions are imposed on the cell boundary and close to the fiber. In our model, the slip effect is considered in the calculation of the efficiency due to inertial impaction and interception. Analytical expressions with slip effect for the efficiency due to inertial impaction are not available.

For a quantitative comparison with the analytical expressions with slip effect, we use formulas in Brown (1993) to compute the pressure drop and filtration efficiency for our nanofiber Sample C. The pressure drop based on the Kuwabara flow with slip effect is (Brown, 1993, Eq. (3.65)):

$$\Delta p = \frac{4\mu\alpha t U_f(1 + 1.996Kn)}{0.25d_f^2[-0.5\ln\alpha - 0.75 + \alpha - \alpha^2/4 + 1.996Kn(-0.5\ln\alpha - 0.25 + \alpha^2/4)]}, \tag{6}$$

where μ is the air viscosity and U_f is the face velocity. The effective nanofiber solidity determined by matching the pressure drop from our simulation to experimental data is $\alpha = 0.059$. This value may not be good for use in the analytical expressions based on the Kuwabara flow. Thus we change α in Eq. (6) and compute Δp for the nanofiber layer, then add on the pressure drop across the substrate measured in experiments, to obtain the total pressure drop. This value is compared to the pressure drop for Sample C measured in experiments. The computed pressure drop matches the experimental value when $\alpha = 0.032$. Therefore, we use $\alpha = 0.032$ as the effective nanofiber solidity for the expressions based on the Kuwabara flow. Brown (1993) listed following expressions for the efficiency due to interception E_R and the efficiency due to diffusion E_D:

$$E_R = \frac{(1 + R)^{-1} - (1 + R) + 2(1 + 1.996Kn)(1 + R)\ln(1 + R)}{2(-0.75 - 0.5\ln\alpha) + 1.996Kn(-0.5 - \ln\alpha)}, \tag{7}$$

$$E_D = 2.27Ku^{-1/3}Pe^{-2/3}(1 + 0.62KnPe^{1/3}Ku^{-1/3}), \tag{8}$$

Table 3
Calculation results for Sample C using analytical expressions (7)–(9)

Particle size (nm)	5	20	50	100	300	780
E_R	0.017	0.075	0.215	0.510	2.18	7.92
E_I	0.00016	0.0019	0.024	0.065	0.318	0.80
E_D	16.1	3.31	1.32	0.724	0.339	0.207
P (calculation) (%)	12.0	68.4	85.9	89.6	79.3	47.0
P (experiment) (%)	26.6	75	88.5	92.2	88.1	61.6

The total penetration across the composite filter P is also computed and compared to experimental data.

where R is the ratio of the particle diameter to the fiber diameter, Pe is the Peclet number. Analytical expressions with slip effect for the efficiency due to inertial impaction are not available. Nevertheless, we use the expression (Stechkina, Kirsch, & Fuchs, 1969) without slip effect to estimate the efficiency due to inertial impaction E_I:

$$E_I = \frac{J \cdot Stk}{(2Ku)^2}, \tag{9}$$

where $J = (29.6 - 28\alpha^{0.62})R^2 - 27.5R^{2.8}$ for $R < 0.4$ and $J = 2.0$ when $R > 0.4$, and Stk is the Stokes number of the particle. The results computed using Eqs. (7)–(9) are listed in Table 3. The nanofiber solidity $\alpha = 0.032$ is used in the calculation and the results should be compared to the experimental data for Sample C. The efficiencies computed from the analytical expressions can be compared to those from our numerical model (Table 2). The efficiency ($E_R + E_I$) from the analytical expressions is significantly larger than E_{I+R} from our numerical model. E_D from the analytical expression is also larger than that from our numerical model except for very small particles. As a result, the penetration from the analytical expressions is lower than that from our simulation for 20–780 nm particles, and is also lower than the experimental data. In the range of 20–780 nm particles, our numerical model gives more accurate prediction for the filtration efficiency than the analytical expressions.

The results in Fig. 6 and Table 2 show that the penetrations measured in experiments are higher than those predicted by the numerical model for particles smaller than 20 nm. They are also higher than the penetrations computed using analytical expressions for particles smaller than 20 nm (Table 3). Podgórski et al. (2006) performed filtration tests for filters with the mean fiber diameter in the range of 0.74–1.41 μm. Their results also showed that the penetrations from experiments were higher than those predicted from filtration theory for very small particles (Podgórski et al., 2006, Figs. 13 and 14). One possible reason for the discrepancy is related to the non-uniformity in fiber sizes and polydispersity of the filter pores. As discussed by Podgórski et al. (2006), the inhomogeneity in the filter structure may lead to zones of higher local porosity and result in higher penetration. Another possible reason is related to our assumption that the nanofiber layer and the substrate act independently to capture particles. The diffusion coefficients of very small particles are large and the range in which the diffusion capture mechanism is effective is wide. Therefore, capture of very small particles by the nanofiber layer and by the substrate may not be independent. This can cause discrepancy between the model and the experimental results.

4. Analysis for the nanofiber filter performance

Our filter testing results show that addition of nanofibers improves the filtration efficiency, but increases the pressure drop at the same time. We use the figure of merit Q to evaluate the overall performance of the nanofiber filters.

We compute Q for Samples A–D and the substrate using the experimental data; the results are plotted as a function of the nanofiber solidity α in Fig. 7. The three curves are for 20, 150 and 780 nm particles. The particle size 150 nm is close to the MPPS, at which the values of Q are expected to be low. Indeed the curve of Q for 150 nm is lower than those for 20 and 780 nm. We make the following observations by comparing the values of Q of Samples A–D and the substrate. (1) The effects of nanofibers on Q are dependent on the particle size. (2) For a small particle size (e.g. 20 nm), the value of Q drops as the nanofiber solidity increases. This is because the increase of the pressure drop outweighs that of the efficiency. (3) For a particle size near the MPPS (150 nm) or a large particle size (e.g. 780 nm), addition of nanofibers can improve Q. The major concern in filter evaluation is the quality at the MPPS and our result confirms that then anofibers can enhance the quality. (4) The value of Q is not a monotonic function of the nanofiber solidity.
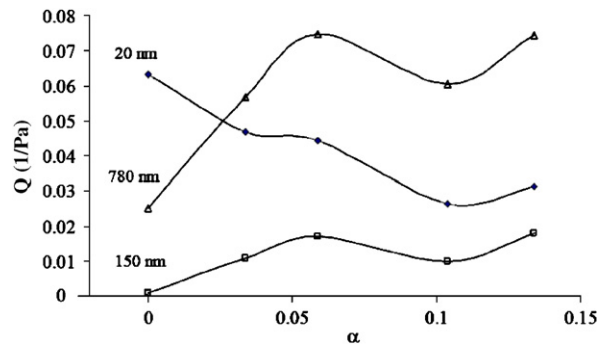
Fig. 7. The figure of merit Q as a function of the nanofiber solidity α. Note that $\alpha = 0.034, 0.059, 0.104$ and 0.134 for Samples D, C, B and A, respectively, and $\alpha = 0$ for the substrate. The three curves are for 20, 150 and 780 nm particles. The face velocity is 10 cm/s for all cases.

Table 4
Characteristic parameters for four standard fiberglass filter media

Parameters	HE1073	HE1021	HF0031	HF0012
Thickness (cm)	0.053	0.069	0.074	0.074
Solidity	0.05	0.049	0.047	0.039
Effective fiber diameter (μm)	1.9	2.9	3.3	4.9
DOP % penetration 0.3 μm at 5.3 cm/s	12.8	39	45.8	79.9
Pressure drop at 5.3 cm/s (mmH$_2$O)	8.4	4.7	3.5	1.3

Sample C with a moderate nanofiber solidity ($\alpha = 0.059$) has the highest Q for 780 nm particles. Sample B has a higher nanofiber solidity ($\alpha = 0.104$) but lower values of Q compared to Sample C. These observations show that the design of nanofiber filters needs to take the particle size in the application into account. It is not always better to add more nanofibers to the filter; there exist optimal nanofiber solidities at which the figure of merit is at maximum.

Kalayci et al. (2006) investigate the figure of merit of nanofiber filters. They argued when solidity increases, the pressure drop increases at a much faster rate than single fiber efficiency due to either diffusion or interception, based on the equations cited by Brown (1993). Therefore, the figure of merit decreases with increased solidity for small particles. For larger particles, it is possible that combined single fiber efficiency due to interception and inertial impaction can increase faster than pressure drop. Their argument agrees qualitatively with our experimental results.

It is of interest to compare the figure of merit of nanofiber filters with those of conventional filters. In Table 4 we list characteristic parameters for four standard fiberglass filter media. The HE type filters are close to HEPA for small particles; the HF type filters are common in HVAC systems. The HE type filters have higher efficiencies than the HF filters. Filtration test results for the standard filter media have been reported in the previous studies (Japuntich et al., 2007; Kim et al., 2007; Wang et al., 2007). Here we compute the figure of merit for them and compare to nanofiber Sample C in Fig. 8. The choice is because Sample C has an effective nanofiber solidity close to the solidity of the standard filters. Sample C shows higher values of Q than the standard filter media for particles larger than 100 nm. For particles smaller than 100 nm, Q of Sample C is between those of HF0031 and HF0012. Among the standard filter media, the HF filters have higher values of Q for particles smaller than 100 nm, whereas the HE filters have slightly higher values of Q for larger particles.

To understand the above results, we use analytical expressions for the pressure drop (6) and filtration efficiency (7)–(9) to compute the figure of merit for both micrometer fibers and nanofibers. We consider four different fiber sizes, 0.15, 0.5, 5 and 20 μm. We also consider a composite filter composed of a layer of 0.15 μm fibers and a substrate of 20 μm fibers. For all the cases, the face velocity is 10 cm/s and the particle density is 1 g/cm^3. The solidity is $\alpha = 0.05$ for all the filters with uniform fiber sizes; it is also 0.05 for the nanofiber layer and for the substrate in the composite filter. The filter thickness is not needed to compute the figure of merit for filters with uniform fiber sizes, but is required for the composite filter. We set the thickness to be 0.15 μm for the single layer 0.15 μm fibers, and 1 mm for the substrate of 20 μm fibers. The pressure drop of the composite filter is the sum of the pressure drops of the nanofiber layer and
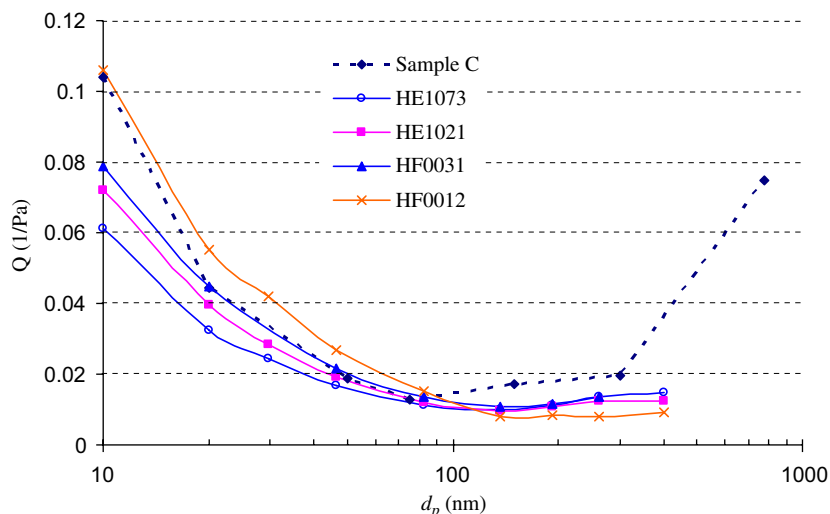
Fig. 8. Figure of merit for the nanofiber filter Sample C and standard fiberglass filter media HE1073, HE1021, HF0031 and HF0012. The face velocity is 10 cm/s for all cases.
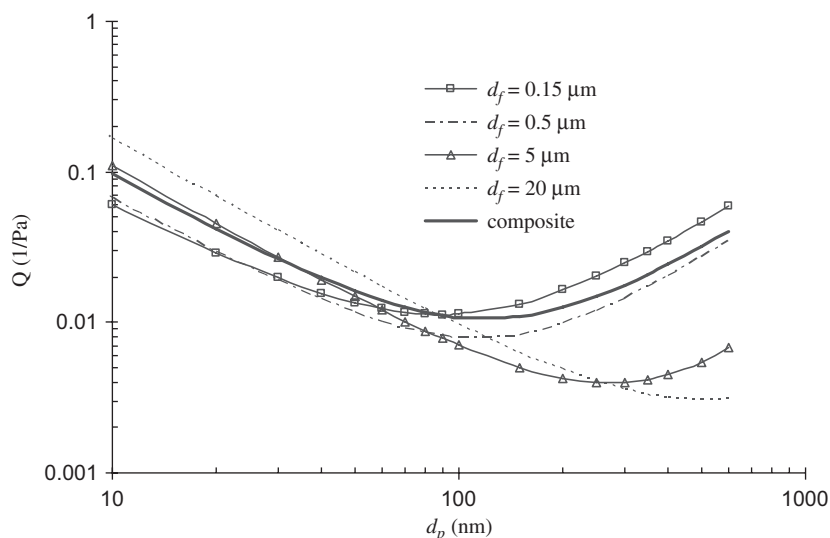

Fig. 9. Figure of merit computed using analytical expressions. Four different fiber sizes, 0.15, 0.5, 5 and 20 μm, and a composite filter composed of a layer of 0.15 μm fibers and a substrate of 20 μm fibers are considered.

the substrate; the penetration of the composite filter is the product of the penetrations of the nanofiber layer and the substrate. The calculated results are shown in Fig. 9. It can be seen that Q for small particles decreases as the fiber size decreases, and Q for large particles increases as the fiber size decreases. The composite filter shows similar Q as the 5 μm fibers for small particles, and higher Q than the 5 μm fibers for large particles. These features agree qualitatively with the experimental data shown in Fig. 8. Therefore, our experimental data can be explained using classical filtration theories.

Podgórski et al. (2006) carried out similar calculation for the figure of merit for fibers down to 0.1 μm. They used analytical expressions for filtration efficiencies due to diffusion and interception with slip effect and omitted the efficiency due to inertial impaction. The expressions they used are slightly different from the ones used by us. Their calculated results agree with ours shown in Fig. 9. Hinds (1998) discussed the effect of fiber size on filter quality,

considering all the mechanical filtration mechanisms without the slip effect. His Fig. 9.12 indicates that the filter quality decreases with decreasing d_f for $d_p < 100$ nm, but increases with decreasing d_f for $d_p > 200$ nm. These results agree well with our experimental data.

Our experimental results and analysis show that decreasing fiber size does not improve the figure of merit for very small particles. On the other hand, nanofiber filters demonstrate better figure of merit for larger than 100 nm compared to conventional fiberglass media. These results provide important guidelines for design of filtration systems.

5. Conclusion

Filters composed of a layer of nanofibers on a substrate made of micrometer fibers are studied. Experimental results show that both the filtration efficiency and the pressure drop increases as the nanofiber solidity increases. We develop a numerical model to simulate the nanofiber filters. The simulation results are in good agreement with experiments for 20–780 nm particles but discrepancies exist for particles smaller than 20 nm. The discrepancies are attributed to the non-uniformity in the filter structures and the breakdown of the assumption that the nanofiber layer and the substrate capture particles independently. The filtration performance of nanofiber filters is evaluated in terms of the figure of merit, which depends strongly on the particle size under consideration and the nanofiber solidity. The figure of merit decreases with increased solidity for small particles; for particles near the most penetrating particle size, increasing nanofiber solidity may improve the figure of merit. We demonstrate that the nanofiber filters have better figure of merit for particles larger than about 100 nm compared to conventional fiberglass filters. For particles smaller than 100 nm, nanofiber filters do not perform better than conventional fiberglass filters.

Acknowledgments

References

Barhate, R. S., & Ramakrishna, S. (2007). Nanofibrous filtering media: Filtration problems and solutions from tiny materials. *Journal of Membrane Science*, *296*, 1–8.

Brown, R. C. (1993). *Air filtration*. London: Pergamon Press.

Davies, C. N. (Ed.). (1973). *Air filtration*. London: Academic Press.

Ellison, C. J., Phatak, A., Giles, D. W., Macosko, C. W., & Bates, F. S. (2007). Melt blown nanofibers: Fiber diameter distributions and onset of fiber breakup. *Polymer*, *48*, 3306–3316.

Friedlander, S. K. (1957). Mass and heat transfer to single spheres and cylinders at low Reynolds numbers. *AIChE Journal*, *3*, 43–48.

George, J. (2007). Nanofiber manufacturing processes for filtration media. In *American filtration & separation society annual conference*. Orlando, Florida, March 2007.

Gradoń, L., Bałazy, A., Podgórski, A. (2006). Nanofibrous media—Promising tools for filtration of nanosized aerosol particles. In *The 7th international aerosol conference*. St. Paul, Minnesota, September 2006.

Graham, K., Ouyang, M., Raether, T., Grafe, T., McDonald, B & Knauf, P. (2002). Polymeric nanofibers in air filtration applications. In *American filtration & separation society annual conference*. Galveston, Texas, April 2002.

Hinds, W. C. (1998). *Aerosol technology* (2nd ed.). New York: Wiley-Interscience.

Japuntich, D., Franklin, L., Pui, D., Kuehn, T., Kim, S. C., & Viner, A. S. (2007). A comparison of two nano-sized particle air filtration tests in the diameter range of 10 to 400 nanometers. *Journal of Nanoparticle Research*, *9*, 93–107.

Kalayci, V., Ouyang, M., & Graham, K. (2006). Polymeric nanofibres in high efficiency filtration applications. *Filtration*, *6*(4), 2006.

Kim, G.-T., Hwang, Y.-J., Lee, C.-G., Cheong, S.-I., Shin, H.-S., Chull, A.-Y., et al. (2006). The performance of nylon 6 nanofilters for removing nano-particles. In *The 7th international aerosol conference*. St. Paul, Minnesota, September 2006.

Kim, S. C., Harrington, M. S., & Pui, D. Y. H. (2007). Experimental study of nanoparticles penetration through commercial filter media. *Journal of Nanoparticle Research*, *9*, 117–125.

Kirsch, A. A., & Stechkina, I. B. (1978). The theory of aerosol filtration with fibrous filters. In D. T. Shaw (Ed.), *Fundamentals of aerosol science.* New York: Wiley.

Lee, K. W., & Liu, B. Y. H. (1980). On the minimum efficiency and most penetrating particle size for fibrous filters. *Journal of the Air Pollution Control Association*, *30*, 377–381.

Lee, K. W., & Liu, B. Y. H. (1982). Theoretical study of aerosol filtration by fibrous filters. *Aerosol Science and Technology*, *1*, 147–161.

Liu, Z. (1993). *Numerical investigation of particle filtration process in fibrous filters*. Ph.D. thesis, University of Wisconsin, Madison.

Natanson, G. L. (1957a). Diffusional precipitation of aerosols on a streamlined cylinder with a small capture coefficient. *Proceedings of the Academy of Sciences of the USSR Physical Chemistry Section*, *112*, 21–25.

Natanson, G. L. (1957b). Diffusional precipitation of aerosols on a streamlined cylinder with a small capture coefficient. *Doklady Akademii Nauk SSSR*, *112*, 100.

Podgórski, A., Bałazy, A., & Gradoń, L. (2006). Application of nanofibers to improve the filtration efficiency of the most penetrating aerosol particles in fibrous filters. *Chemical Engineering Science*, *61*, 6804–6815.

Stechkina, I. B. (1966). Diffusion precipitation of aerosols in fiber filters. *Doklady Academii Nauk SSSR*, *167*, 1327.

Stechkina, I. B., Kirsch, A. A., & Fuchs, N. A. (1969). Studies on fibrous aerosol filters—IV. Calculation of aerosol deposition in model filters in the region of maximum penetration. *Annals of Occupational Hygiene*, *12*, 1–8.

Subbiah, T., Bhat, G. S., Tock, R. W., Parameswaran, S., & Ramkumar, S. S. (2005). Electrospinning of nanofibers. *Journal of Applied Polymer Science*, *96*(2), 557–569.

Wang, J., Chen, D. R., & Pui, D. Y. H. (2007). Modeling of filtration efficiency of nanoparticles in standard filter media. *Journal of Nanoparticle Research*, *9*, 109–115.